NANO: Brief Reports and Reviews
Vol. 14, No. 1 (2019) 1950014 (6 pages)

DOI: 10.1142/S1793292019500140

World Scientific
www.worldscientific.com

Green Hydrothermal Synthesis of Fluorescent Carbon Dots from Glucose and Taurine for Fe^{3+} and pH Sensing

Yanmin Xu, Lihe Yan*, Mengmeng Yue and Yang Yu
Key Laboratory for Physical Electronics and Devices of the Ministry of Education and Shaanxi Key Lab of Information Photonic Technique School of Electronics and Information Engineering Xi'an Jiaotong University Xi'an 710049, P. R. China
**liheyan@mail.xjtu.edu.cn*

Received 26 July 2018
Accepted 7 December 2018
Published 15 January 2019

Carbon nanodots (C-dots), as a class of heavy-metal-free fluorescent nonmaterial have drawn increasing attention due to their strong photoluminescence (PL), good biocompatibility and low toxicity. Herein, we synthesize nontoxic fluorescent C-dots by hydrothermal treatment of the mixture of glucose and taurine, in which process the formation and the surface passivation of C-dots take place simultaneously. The influence of reaction temperature, reaction time and feed ratio of glucose to taurine on the PL property of C-dots is studied. As the C-dots exhibit sensitive pH and iron ion dependent PL property, they can be used for pH and Fe^{3+} sensing in solutions.

Keywords: Carbon materials; nanoparticles; optical materials and properties.

1. Introduction

During the past decades, luminescent quantum dots (QDs) have attracted considerable interests due to their unique optical and electronic properties.[1–3] The traditional semiconductor QDs such as CdS QDs and CdSe QDs, more or less, suffer from the problems of toxicity and hydrophobicity, limiting their practical applications.[4] Fluorescent carbon dots (C-dots) have attracted great attention due to their favorable luminescent properties, low toxicity, biocompatibility and easy functionalization.[5–8] They have found many applications in biology imaging, medicine delivery and biosensing areas. Until now, many synthesis strategies of C-dots have been reported, such as laser ablation, arc discharge, hydrothermal treatment and microwave methods,[9–14] Among these methods, hydrothermal synthesis route based on water system has been widely used due to its unique advantages of easy-operation, low cost and high efficiency.[13]

Using the hydrothermal synthesis method, C-dots with various PL properties and applications have been prepared.[15–18] For instance, Qu *et al.* fabricated carbon nanoparticles (CNPs) via a hydrothermal synthesis route, which were used for Fe^{3+} and dopamine sensing.[18] Tong *et al.* fabricated N and S co-doped carbon QDs for the detection of Fe^{3+} and L-cysteine.[19] Guo and co-workers

*Corresponding author.

prepared carbon dots (C-dots) with tunable emissions ranging from blue to near-infrared region using polythiophene derivatives.[20] It's believed that compounds containing both amino and carboxyl groups are beneficial to synthesize C-dots with high PL quantum yield.[21] However, to some extent, the usage of some materials containing amino groups might cause toxicity of the products. Based on this consideration, materials abundant in amino groups may be a suitable precursor. Taurine, as a kind of humans' essential amino-acid, is helpful in promoting the development of nervous system and enhancing the cardiovascular function. Due to its intrinsic features of abundance in amino groups, nontoxicity and easy access, taurine can be a potential candidate to prepare nontoxic luminescent C-dots.

In this work, we have developed a simple and green approach to synthesis the C-dots through hydrothermal treatment of glucose and taurine. The influence of reaction temperature, reaction time and mass ratio on the PL property of C-dots is studied. The optical properties and chemical structures are characterized by UV–Vis absorption spectroscopy, PL, Fourier transform infrared (FTIR) spectroscopy, X-ray photoelectron spectroscopy (XPS) and transmission electron microscope (TEM). As these C-dots exhibit pH- and iron ion-sensitive PL property, their potential applications in pH and Fe^{3+} sensing of solutions are demonstrated.

2. Experimental

C-dots are prepared by hydrothermal treatment of the mixture of glucose and taurine. About 2 mg glucose and taurine with different ratios are added into 30 mL distilled water, and then mixed uniformly by ultrasonic treatment. The mixture is then moved to a 50 mL Teflon-lined autoclave and heated in an oven for reaction at 150°C for 1–3 h. After that, the obtained brown-yellow solution is naturally cooled down to room temperature, and then centrifuged at 12 000 rpms for 10 min to remove the black precipitates. Finally, the yellow supernatant is collected for further characterizations and applications.

A typical procedure for the detection of Fe^{3+} is described as follows: Different amounts of Fe^{3+} ions which are added into 2 mL of the C-dots solution to obtain mixtures with concentrations ranging from 1 μM to 700 μM. The fluorescence spectrum of pristine C-dots is examined and the intensity is recorded as F_0, while those for the mixture with Fe^{3+} are recorded as F. The ratio changes of F to F_0 (F/F_0) are plotted as a function of the Fe^{3+} concentrations. To confirm the selectivity of Fe^{3+} sensing, the influence of other metal ions (Mg^{2+}, K^+, Ca^{2+}, Cu^{2+}, Zn^{2+}, Ag^+, Na^+, Ni^{2+}, Pb^{2+}, Sn^{2+}) on the PL intensity are studied.

For pH sensing, a series of standard pH buffers are prepared with distilled water by adding different amount of NaOH or H_3PO_4. Then, the C-dots solutions are mixed with the buffer solutions with varied pH values. The final mixture keeps the same volume to reduce the error of dilution ratio. After shaking, the fluorescence spectra are recorded at varied pH values. All the detection experiments are carried out under the same conditions at room temperature.

3. Results and Discussions

Figure 1(a) shows the TEM and high-resolution TEM (HRTEM) images of the C-dots. The as-prepared C-dots distribute on the copper grid homogeneously, and no large aggregations are observed, indicating that the C-dots are well dispersed in water. The mean size of the C-dots is estimated to be about 3 nm [as shown by the inset of Fig. 1(a)]. The HRTEM image of the C-dots shows well-resolved crystal lattice fringes with a spacing of 0.21 nm, which is very close to the (100) facet of graphite carbon.[9] Figure 1(b) shows the UV–Vis and fluorescence spectra of the C-dots solution. It is seen that there is a wide absorption tail above 260 nm, which could be attributed to the π–π^* transition of aromatic sp^2 domains and n–π^* transition of C=O band.[22] The C-dots exhibit a fluorescence peak at 410 nm under 340 nm excitation as shown by the red line in Fig. 1(b).

To find the optimal reaction conditions, we investigate the influence of reaction temperature, reaction time and feed ratio of glucose to taurine on the PL property of C-dots. Figures 1(c)–1(e) show the PL intensity under 340 nm excitation at different reaction temperature, reaction time and mass ratio, respectively. The reaction temperature is one of the most important factors on the formation of the C-dots during the hydrothermal reaction. As shown in Fig. 1(c), with increasing the reaction temperature, the fluorescence of C-dots is gradually heightened, and the optimum takes place at 150°C.

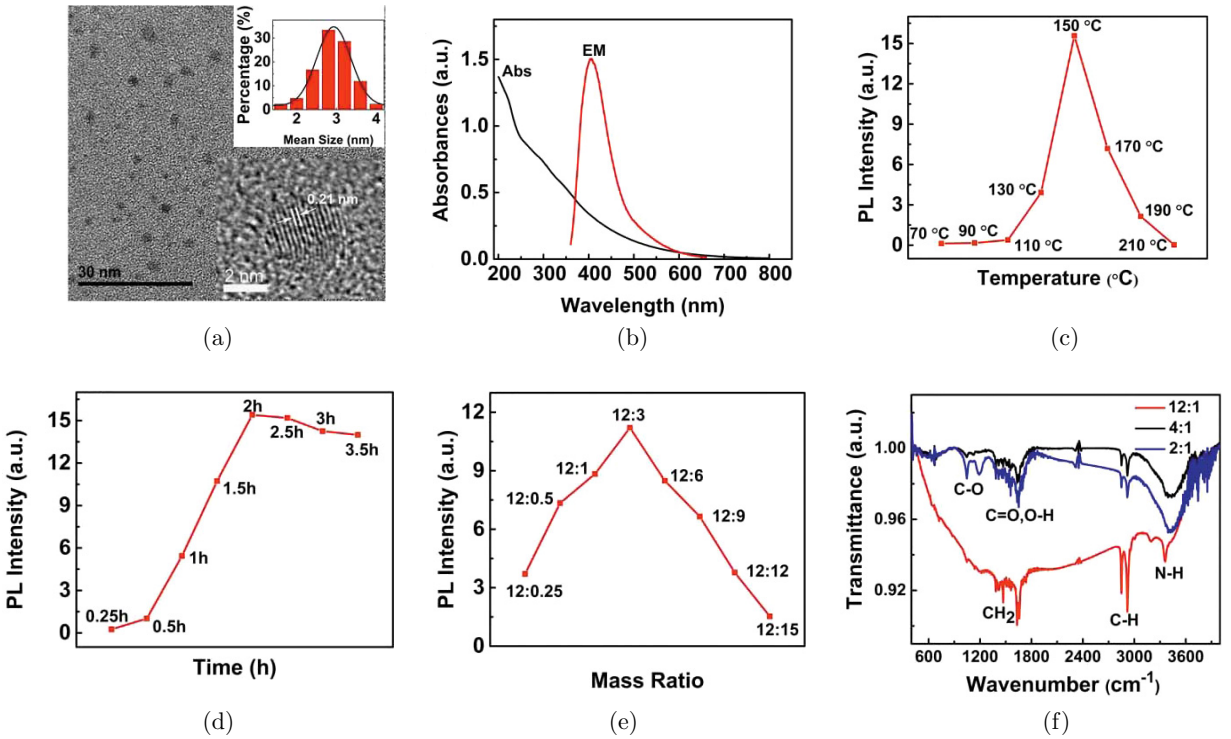

Fig. 1. (a) TEM image (the insert is the size distribution and HRTEM image), (b) UV-Vis absorption and PL (under 340 nm excitation) spectra. The dependence of PL intensity on (c) reaction temperature, (d) reaction time, and (e) mass ratio. (f) FTIR spectra of the as-prepared C-dots with different mass ratio (color online).

When the temperature exceeds 150°C, the fluorescence of the C-dots declined rapidly, which may be related to the nonluminous functional groups.[23] Hence, 150°C heating is employed in the following experiments. Similarly, the PL intensity is optimized when the reaction time is adjusted to 2 h, and the ratio of glucose to taurine is adjusted to 4:1. The quantum yield of the C-dots prepared in the optimum conditions is estimated to be 11%.

Figure 1(f) shows the FTIR spectra of C-dots prepared with different feed ratio. Stretching vibrations of N–H bond at 3360 cm^{-1}, C–H bond at 2900 cm^{-1}, bending vibrations of CH_2 at 1470 cm^{-1}, vibrational absorption band of C=O/O–H bond at 1630 cm^{-1} and the C–O bond around 1000–1200 cm^{-1} are observed.[22] The results reveal that there are abundant functional groups such as amino and carboxyl groups on the surface. By comparing the FTIR spectra under different mass ratios, we find that the amount of the functional groups increases with increasing taurine. Because the PL emission of C-dots arises mainly from the radiative recombination of electron and holes located at the surface energy traps, the amount of the function groups plays an important role on the PL intensity.[24] When the ratio changes from 12:1 to 4:1, the increase of the luminescent functional groups will cause the enhancement of PL intensity. However, when the amount of taurine is further increased, too many nonluminescent functional groups will be induced and the PL intensity decreases due to the competition of the radiative and nonradiative recombination processes. The influence of the reaction time on the PL intensity can be also interpreted using this mechanism, in which longer reaction time will increase the luminescent groups, while too long time will introduce too many nonluminescent groups decreasing the PL intensity.

To further confirm the compositions of the C-dots, XPS survey is performed. As shown in Fig. 2(a), the XPS spectrum shows three peaks at 284.74 eV, 398.80 eV and 532.67 eV, which are attributed to C1s, N1s and O1s, respectively. The high-resolution C1s spectrum [Fig. 2(b)] shows three peaks including C=C/C–C at 284.3 eV, C–O at 285.6 eV and C–N at 287.2 eV. The deconvolution of high-resolution N1s [Fig. 2(c)] spectrum indicates the presence C–N–C peak centered at 398.4 eV

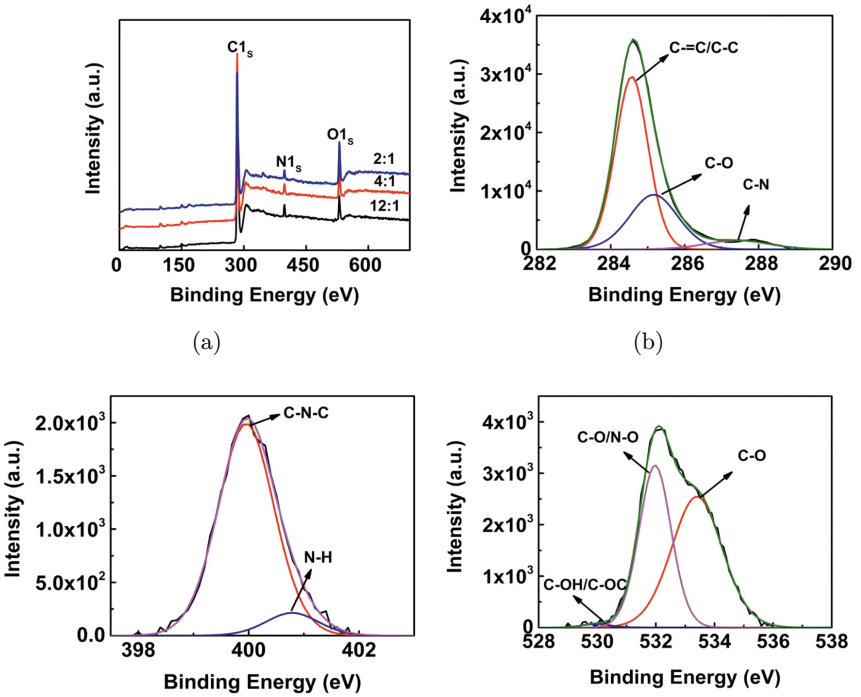

Fig. 2. (a) XPS spectra of the C-dots. High-resolution XPS spectra of (b) C 1s, (c) N 1s and (d) O 1s peaks of the C-dots, respectively (color online).

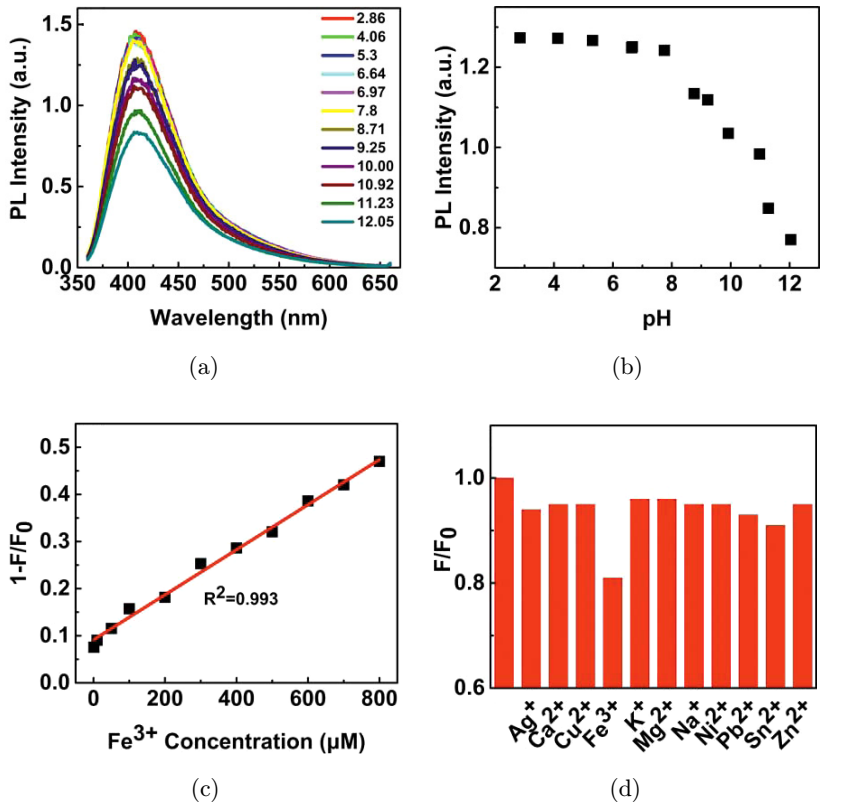

Fig. 3. (a) PL spectra of the C-dots at different pH. The dependence of PL intensity on (b) pH and (c) Fe^{3+} concentration. (d) Comparison of PL intensity in the presence of various metal ions (color online).

and N–H peaks at 401.6 eV. C–O, C–O–C and N–O peaks can be seen in the O1s spectrum [Fig. 2(d)], which is centered at 533.2 eV, 530 eV and 531.9 eV, respectively. Consistent with the analysis of FTIR spectra, the XPS spectra also confirm the presence of a huge number of multiple oxygen and amine groups on the surface of the C-dots.

To demonstrate the ability of pH sensing of the C-dots, we measure the fluorescence spectra at different pH values. The PL intensity decreases with increasing the pH from 2.86 to 12.05 as shown in Fig. 3(a). Figure 3(b) depicts the PL intensity as a function of the pH values. It shows that the emission intensity decreases slowly from pH = 2.86 to pH = 6.97 and then decreases dramatically from pH = 7.8 to pH = 12.05. The lowest detection limit is estimated to be less than 0.33 based on our experimental results. The pH dependence of the PL intensity could be attributed to the aggregation of C-dots. With increasing pH value, the C-dots are easily aggregated to larger particles due to some noncovalent molecular interactions, such as hydrogen bonds between the carboxyl groups. The aggregation of C-dots will cause the red shift of the absorption peak and thereby the decrease of the PL intensity in the blue light region.[25]

Figure 3(c) shows the influence of the Fe^{3+} concentration on the PL intensity of the C-dots. To evaluate the sensitivity of Fe^3 sensing, we examine the fluorescence intensity ratio (F/F_0) change for different Fe^{3+} concentrations. By increasing the Fe^{3+} concentration from 1 μM to 700 μM, the value of $1 - F/F_0$ increases almost linearly. The fitted solid curve in Fig. 3(c) shows a correlation coefficient of 0.993, and the limit of detection is estimated to be less than 1 μM. To evaluate the selectivity of this sensing system, we examine the PL intensity changes in the presence of different metal ions including Ag^+, Na^+, Ni^{2+}, Pb^{2+}, Sn^{2+}, Ca^{2+}, Mg^{2+}, Zn^{2+}, K^+ and Cu^{2+} under the same conditions. As shown in Fig. 3(d), Fe^{3+} ions show the greatest quenching effect on fluorescence among the metal ions, indicating the excellent Fe^{3+} sensing properties of the C-dots. The fluorescence quenching by Fe^{3+} ions is ascribed to nonradiative electron transfer involving partial transfer of electrons in excited state to the d orbital of Fe^{3+}.[26] Due to the nontoxic feature of as-prepared C-dots, their high sensitivity to pH and Fe^{3+} can be used in the some biosensing areas such as *in-vivo* imaging and human hemoglobin detection.

4. Conclusions

In summary, we report a simple and green approach to synthesize the C-dots through hydrothermal treatment of glucose and taurine. The influence of reaction temperature, reaction time and feed ratio of glucose to taurine on the PL property of C-dots is studied. As these C-dots exhibit pH and iron ion-sensitive PL property, their potential applications in pH and Fe^{3+} sensing of solutions are demonstrated.

Acknowledgments

This work was supported by National R&D Program of China (2017YFA0207400), the National Natural Science Foundation of China (Grant Nos. 11674260 and 11474078), the Fundamental Research Funds for the Central Universities, and the collaborative Innovation Center of Suzhou Nano Science and Technology.

References

1. S. Zhu, N. Meng, L. Wang, J. Zhang, Y. Song, H. Jin, K. Zhang, H. Sun, H. Wang and B. Yang, *Angew. Chem.* **125**, 4045 (2013).
2. S. Qu, X. Wang, Q. Lu, X. Liu and L. Wang, *Angew. Chem.* **51**, 12215 (2012).
3. M. Strasser, K. Setoura, U. Langbein and S. Hashimoto, *J. Phys. Chem. C* **118**, 25748 (2014).
4. Y. Chen and Z. Rosenzweig, *Anal. Chem.* **74**, 5132 (2002).
5. C. Shen, L. Su, J. Zang, X. Li, Q. Lou and C. Shan, *Nanoscale Res. Lett.* **12**, 447 (2017).
6. B. Wang, W. Tang, H. Lu and Z. Huang, *J. Mater. Sci.* **50**, 5411 (2015).
7. P. Namdari, B. Negahdari and A. Eatemadi, *Biomed. Pharmacother.* **87**, 209 (2017).
8. L. Zhao, L. Fan, M. Zhou, H. Guan, S. Qiao, M. Antonietti and M. Titirici, *Adv. Mater.* **22**, 5202 (2010).
9. N. Vanthan, L. Yan, J. Si and X. Hou, *J. Appl. Phys.* **117**, 084304 (2017).
10. D. Zhang, B. Goekce, C. Notthoff and S. Barcikowski, *Sci. Rep.* **5**, 13661 (2015).
11. Y. Ma, H. Ren, J. Si, X. Sun, H. Shi, T. Chen, F. Chen and X. Hou, *Appl. Surf. Sci.* **261**, 722 (2016).
12. J. Si and K. Hirao, *Appl. Phys. Lett.* **91**, 91105 (2007).
13. S. Liu, J. Tian, L. Wang, Y. Zhang, X. Qin, Y. Luo, M. Abdullah, O. Abdulrahman and X. Sun, *Adv. Mater.* **24**, 2037 (2012).

14. R. Delfino, C. Marco, C. Miguel, M. Miguel, W. Duncan, S. Greg, Z. Wang and N. Arup, *Nanoscale Res. Lett.* **11**, 424 (2016).
15. X. Liu, T. Li, Q. Wu, X. Yan, C. Wu, X. Chen and G. Zhang, *Talanta* **165**, 216 (2017).
16. R. Wang, X. Wang and Y. Sun, *Sens. Actuators B, Chem.* **241**, 73 (2017).
17. W. Liu, H. Diao, H. Chang, H. Wang and T. Li, *Sens. Actuators B, Chem.* **241**, 190 (2017).
18. H. Wu, J. Jiang, X. Gu and C. Tong, *Microchim. Acta.* **184**, 2291 (2017).
19. K. Qu, J. Wang, J. Ren and X. Qu, *Chem. Eur. J.* **19**, 7243 (2013).
20. L. Guo, J. Ge, W. Liu, G. Niu, Q. Jia, H. Wang and P. Wang, *Nanoscale* **8**, 729 (2016).
21. P. Hsu and H. Chang, *Chem. Commun.* **48**, 3984 (2012).
22. H. Xu, L. Yan, V. Nguyen, Y. Yu and Y. Xu, *Appl. Surf. Sci.* **414**, 238 (2017).
23. Y. Liu and Q. Zhou, *Int. J. Environ. Anal. Chem.* **97**, 1113 (2017).
24. N. Vanthan, J. Si, L. Yan and X. Hou, *Carbon* **95**, 659 (2015).
25. C. Wang, Z. Xu, H. Cheng, H. M. G. Lin and C. Zhang, *Carbon* **82**, 87 (2015).
26. N. Vanthan, L. Yan, J. Si and X. Hou, *Opt. Mater. Express* **6**, 312 (2016).